POLSKA AKADEMIA NAUK

INSTYTUT MASZYN PRZEPŁYWOWYCH

TRANSACTIONS OF THE INSTITUTE OF FLUID-FLOW MACHINERY

PRACE INSTYTUTU MASZYN PRZEPŁYWOWYCH

105

GDAŃSK 1999

THE TRANSACTIONS OF THE INSTITUTE OF FLUID-FLOW MACHINERY

exist for the publication of theoretical and experimental investigations of all aspects of the mechanics and thermodynamics of fluid-flow with special reference to fluid-flow machines

*

PRACE INSTYTUTU MASZYN PRZEPŁYWOWYCH

poświęcone są publikacjom naukowym z zakresu teorii i badań doświadczalnych w dziedzinie mechaniki i termodynamiki przepływów, ze szczególnym uwzględnieniem problematyki maszyn przepływowych

Wydanie publikacji zostało dofinansowane przez PAN ze środków DOT uzyskanych z Komitetu Badań Naukowych

EDITORIAL OFFICE – REDAKCJA

Wydawnictwo Instytutu Maszyn Przepływowych
Polskiej Akademii Nauk
ul. Gen. Józefa Fiszera 14, 80-952 Gdańsk, skr. poczt. 621,
☎ (0-58) 341-12-71 wew. 141, fax: (0-58) 341-61-44,
e-mail: esli@imppan.imp.pg.gda.pl

ISSN 0079-3205

TRANSACTIONS OF THE INSTITUTE OF FLUID-FLOW MACHINERY

No. 105, 1999, 17-32

WITOLD ELSNER,[1], STANISŁAW DROBNIAK[1]

Phase-reconstruction of a moving cylinder wake

The paper presents a consecutive stage of research devoted to modelling of nonstationary rotor-stator interaction in plane cascade flows. Measurements performed with the help of a hot-wire and supplemented by phase-averaged technique allowed to reconstruct the velocity field in the wake behind the moving cylinder. The results obtained confirm that the flow behind the moving cylinder is dominated by the Karman vortex street forming in a repetitive manner. Triggering of the Karman vortex street which takes place when the moving cylinder passes the shear layer, has been proven in a direct way i.e. by phase – reconstructed pictures of velocity field.

1. Introduction

The main source of the flow unsteadiness in turbomachinery blading is the so-called rotor-stator interaction. This complex flow phenomenon consists of two separate effects, namely the viscous and the potential interactions.

The viscous interaction is caused by stator wakes that produce the circumferential nonuniformity of the flow-field in the axial gap, which are then cut by the rotor blades. The potential interaction reveals itself as the flow periodicity induced by the moving rotor blades, which would exist even if the fluid was an inviscid one. The latter effect can cause unsteadiness in both the upstream and downstream directions and its influence decays rapidly with the increase of an axial gap. The viscous wake interaction convected downstream of the wake - generating device is much more durable than the previous one and that is why it is a point of interest of numerous scientific papers.

The most common method of simulation of nonstationary rotor-stator interaction in linear cascade experiments is to introduce moving rods, rotating upstream the test cascade as it has been described among the others by Adachi and Murakami (1979). At the inlet of compressor stator blades they applied a rotor wheel with cylindrical bars, and its rotation was assumed to simulate the interaction of

[1]Institute of Thermal Machinery Technical University of Częstochowa, Al. Armii Krajowej 21, 42-200 Częstochowa

the real rotor blades. The design of an experimental stand allowed to compare a 3D flow within the blade passages both for the steady and periodically disturbed inflow. Measurements were performed at a midspan in a stationary frame of reference with the use of the rotating, single-wire hot-sensors. The phase-averaged procedure made it possible to determine the time-dependent periodic velocity component with the simultaneous of velocity oscillations damping, induced by the Karman vortex path behind the moving cylinders.

Another interesting experimental analysis of the unsteady three-dimensional flow and pressure field in an annular compressor cascade with an upstream rotor has been described by Schulz et al. [10] and Gallus et al [8]. Rotor-stator viscous interaction was generated by a rotor, which consisted of 24 cylindrical rods, simulating the rotor blades. The wake-flow pattern behind the rotating cylinders was also examined by Wierciński [11] and later on by Poengsen and Gallus [9] as well as by Wood et al. [13]. A similar technique was used by Dullenkopf et al. [5] in the research concerning the augmentation of a heat transfer along the surface of a convectively cooled gas turbine blade. In their research the wake – generator consisted of a disc equipped with cylindrical bars and their rotation upstream of the cascade was supposed to simulate the effect of moving rotor blades.

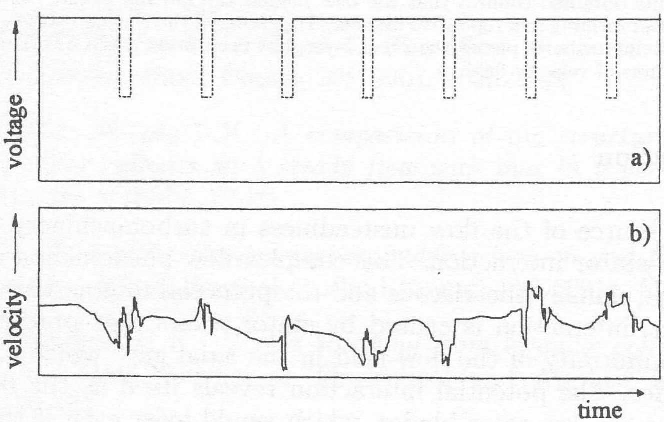

Fig. 1. The sample record of a reference signal (a) and velocity signal (b).

The credibility of simulation of nonstationary rotor-stator interactions by means of rotating cylindrical rods has been questioned by Bogusławski and Elsner [2, 7] and also quite recently by Wysocki et al. [14]. It has been shown in the above papers that application of the rotating rods as the simplest solution may be misleading, when the two processes i.e. wake and vortex street are phase-correlated. The consequences of the above state may be quite serious as it has been proved in Wysocki et al. [14]. Fig. 1 taken from this paper presents a sample velocity time record registered behind a row of moving cylindrical bars. The velocity signal recorded by a single hot-wire (trace b) was accompanied by phase reference signal (trace "a") which marked the position of consecutive rods.

As can be seen the velocity signal does not exhibit any trace of periodicity and furthermore this observation is fully confirmed by the data plotted in Fig. 2. The value of the overall velocity variance $\overline{C*^2} = \overline{\widetilde{C}^2} + \overline{c'^2}$ attains a constant value at $N = 40$ recorded periods, while the periodic variance $\overline{\widetilde{C}^2}$ appears to be a monotonic decreasing function of the N number. At the same time the shape of a phase averaged velocity profile $< c(t) >$ (not shown here) tends to a practically constant value without any symptoms of flow periodicity. One may conclude therefore that mutual correlation between the cylinder motion and vortex street gives the velocity field where the results of measurements may depend on their location in reference to the vortex trajectories and one should treat these results with caution.

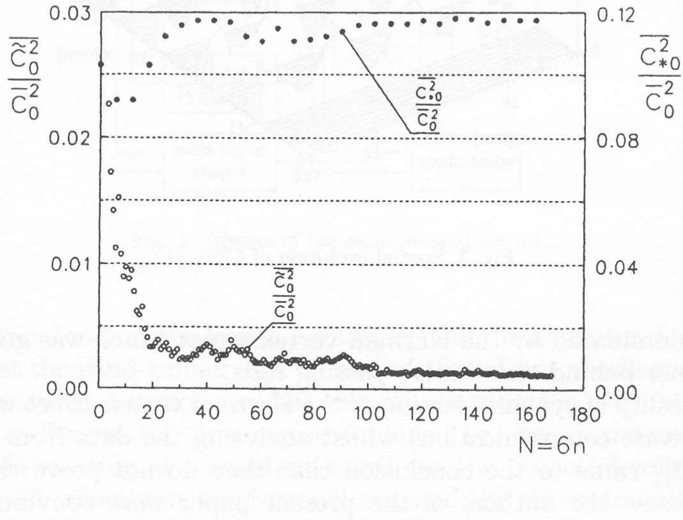

Fig. 2. The distribution of overall and periodic velocity variance.

The most probable explanation of the above phenomenon i.e. the phase-correlation between the wake and the Karman vortex street received however only the indirect confirmation in the papers discussed above. In particular it has been shown that phase-average velocity variance showed a distinct periodicity in the direction parallel to the direction of the cylinder motion and it was believed that the lines connecting the variance maxima determined a direction of the vortex trajectories as presented in Fig. 3 (Bogusławski and Elsner [2]). The angle between vortex trajectories and the direction of the main flow allowed to evaluate a vortex convection velocity that is very close to the one observed for Karman vortex streets behind a stationary cylinder. The distances between vortex trajectories were also very close to the predicted value, if one assumed Strouhal number characteristic to the vortex street behind circular cylinder equal 0.2. These arguments suggested that the flow structure behind the cylinder crossing a potential

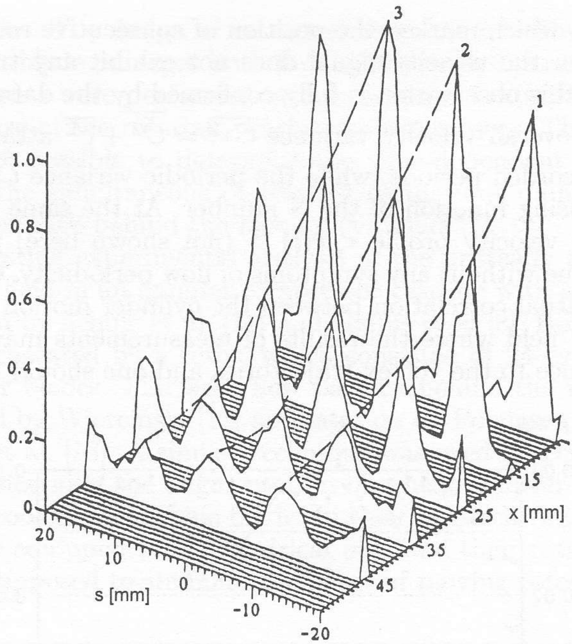

Fig. 3. Spatial evolution of $\overline{\widetilde{C}_a^2}(x, s)$.

jet core was dominated by the Karman vortex street which was generated in repetitive manner behind consecutive passing rods.

The possibility of synchronisation of the Karman vortex street was questioned by Wood (private communication) whilst analysing the data from (Bogusławski and Elsner [2]) came to the conclusion that they do not prove the above phenomena. Because the authors of the present paper were convinced about the correctness of their observations presented in (Bogusławski and Elsner [2]) so the proper set of experimental research was conducted in order to clarify the above arguments.

2. Experimental facility and data processing techniques

In order to verify the existence of mutual correlation between the wake position and Karman vortex street it was decided to recover the unsteady velocity field behind a moving cylinder from the phase-locked X-wire measurements without using the Taylor hypothesis. To obtain a proper resolution of phase-averaged velocity field the above measurements were performed on a very fine grid of measuring points.

The measurements have been performed with the use of a test facility which is schematically presented in Fig. 4. The disturbance generator consisted of a disc

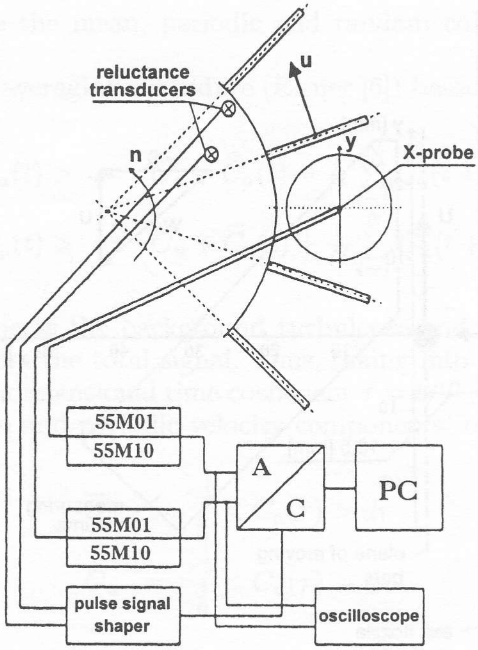

Fig. 4. Scheme of the experimental set-up.

with 10 cylindrical rods of the length $l = 90$ mm and the diameter $d = 3mm$ which was installed at the wind-tunnel exit. The wind-tunnel exit nozzle with a diameter $D = 80$ mm ensured a uniform radial velocity distribution $C(r) = const$ at the exit plane as well as in the flow region occupied by the jet potential core. The cylindrical rods rotating at a constant speed cut the potential core at 90-degree angle. The outlet velocity at wind-tunnel exit and the circumferential velocity of cylinders was kept constant at the level $C = U = 8$ m/s.

To measure the wake behind a moving cylinder the X hot-wire probe and two-channel DISA 55M System coupled with PC computer has been applied. The signals from both channels have been sampled in a 12-bit A/D converter at the rate $f = 8$ kHz. The sampling process was started by a signal from a reluctance transducer, which served as a key-phasor. Contrary to the previous experiment where each cylinder was generating the phase reference signal it was decided to perform the measurement behind one and only one cylindrical rod. One could expect that such a choice should reduce the random scatter of velocity traces recorded behind the different cylinders. That is why the two reluctance transducers have been applied with the first starting and the second ending the data acquisition process.

The 1001 measuring points have been evenly distributed in a measuring volume as it is shown schematically in Fig. 5. The main axis of the measuring plane was placed at an angle 45^o degree to the axis of an aerodynamic wake, i.e. it was

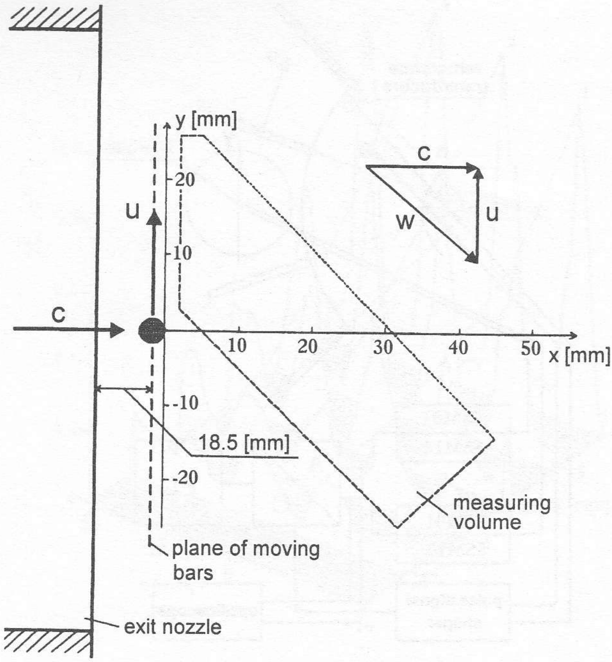

Fig. 5. Localisation of the measuring area in reference to the wind-tunnel exit.

parallel to W velocity vector. The width of the measuring area has been adjusted according to Bogusławski and Elsner [2], and contained at least one full width of a moving vortex street. A trustworthy reconstruction of a moving wake would require simultaneous measurements in all measuring points. It is obvious however, that the presence of a large number of velocity transducers would distort the analysed velocity field. That is why in the present experiment the single X-wire probe has been applied. The phase-locked measurements enabled the reconstruction of the velocity field generated by a moving cylinder crossing the shear layer. This reconstruction was possible provided that a moving circular cylinder entering the potential core generated the Karman vortex street in a repetitive manner, i.e. the first vortex in the flow field was formed always almost in the same place.

The phase-averaging of the signals recorded by X-wire probe enabled to calculate the time series of velocity components in the circumferential C_u and axial C_a directions. Following the triple decomposition idea (Elsner [6]) the instantaneous values of both axial and circumferential absolute velocity components could be expressed by the formulae:

$$\begin{aligned} C_a(t) &= \overline{C}_a + \widetilde{C}_a(t) + c'_a(t) \\ C_u(t) &= \overline{C}_u + \widetilde{C}_u(t) + c'_u(t) \end{aligned} \quad . \qquad (2.1)$$

where $\overline{C}, \widetilde{C}, c'$ denote the mean, periodic and random components of absolute velocity vector.

The phase-locked averaging procedure (Elsner [6]) based on the relationships

$$\begin{aligned} < C_a(t) > &= \overline{C}_a + \widetilde{C}_a(t) + \frac{1}{N}\sum_{i=1}^{N} C_a(t+iT) \\ < C_u(t) > &= \overline{C}_u + \widetilde{C}_u(t) + \frac{1}{N}\sum_{i=1}^{N} C_u(t+iT) \end{aligned} \tag{2.2}$$

where $T = 60/zn$, rejects the background turbulence and extracts only the deterministic motion from the total signal. Thus, taking into account (2.2) in (2.1) and introducing a nondimensional time coefficient $\tau = t/T$ $(t \in (0,T), \tau \in (0,1))$, one may get the mean and periodic velocity components, respectively

$$\begin{aligned} \overline{C}_a &= \int_0^1 < C_a(\tau) > d\tau \\ \overline{C}_u &= \int_0^1 < C_u(\tau) > d\tau \end{aligned} \tag{2.3}$$

$$\begin{aligned} \widetilde{C}_a(\tau) &= < C_a(\tau) > -\overline{C}_a \\ \widetilde{C}_u(\tau) &= < C_u(\tau) > -\overline{C}_u \end{aligned} \tag{2.4}$$

It should be noticed here, that contrary to our previous paper (Bogusławski at al. [3]) the mean velocity components have been subtracted in the above relations. It means therefore, that the observer watching the oscillatory flow field is no longer placed in the centre of vortex, but it moves with the mean velocity vector instead.

3. Preliminary tests of experimental data

During the experiment the measurements of velocity field have been performed at 1001 measuring points. The hot wire signals registered in consecutive wake passages behind the selected cylinder were sampled at a rate equal 8 kHz, that for the given values of measuring parameters gave 100 samples for one wake passage. It means therefore that the results obtained allowed to trace 100 time stages of nonstationary velocity field behind the moving cylinder.

During the preliminary experiment it was necessary to determine the minimum number of periods needed to perform trustworthy phase-averaging procedure. Sample stability tests for axial and circumferential velocity components have been presented in Figs. 6 and 7 respectively. As can be seen both first and second order statistical moments became stable for $N = 50$ and this value has been applied for further research.

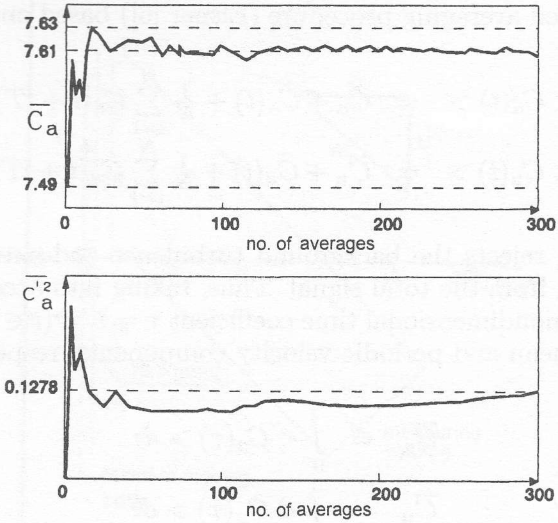

Fig. 6. The sample stability test for axial velocity component.

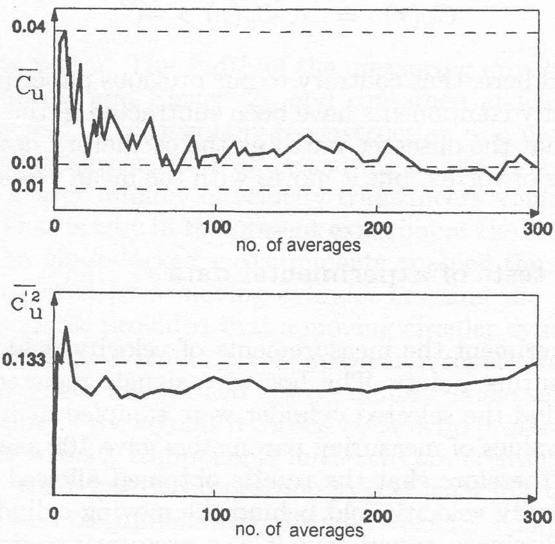

Fig. 7. The sample stability test for circumferential velocity component.

4. Computer aided visualisation of oscillatory velocity component

The detailed insight into the internal structure of the periodic velocity field induced by the passage of the vortex may be obtained from the velocity maps of periodical velocity components. As it has been stated above the oscillatory components $\widetilde{C}_a, \widetilde{C}_u$ have been obtained by subtracting the mean value from the total signal in accordance to equations (2.4) whereas the magnitude $|C|$ and direction α of particular velocity vectors has been determined according to the following formulae

$$\begin{aligned} |C| &= \sqrt{\widetilde{C}_a^2(t) + \widetilde{C}_u^2(t)}|_{\tau=idem} \\ \alpha &= \arctan \frac{C_u(t)}{C_a(t)}|_{\tau=idem} \end{aligned} \tag{4.1}$$

The resulting phase-averaged velocity fields have been presented in Figs. 8, 9 where one may notice well defined distortions of velocity field caused by passing vortices. As can be seen the most regular pattern is observed for the initial area of the wake, where the vortices maintain their maximum spatial coherence while in the region placed further downstream the intensity of rotation and degree of spatial coherence is much weaker as indicated by smaller lengths of velocity vectors.

One should also notice that the spatial coherence of the vortices is preserved only in the inner region of the jet where the clear pattern of oscillatory velocity field may be observed (see Fig. 8) . In the outer region of the wake the oscillatory flow field is almost non-traceable which suggests that the phase-relationship is not preserved in this area. This observation agrees with the statements concerning the round free jet made by Crow and Champagne [4] who have noticed "the short-lived nature" of the outer part of coherent vortices which may be attributed to their interactions with the irregular outer structures which are not phase-linked with the proper coherent vortices. One may expect however, that the phase-averaging procedure cancels all these random phenomena that in turn results in much smaller amplitudes of oscillatory velocity components in the outer region of the wake.

The distance between particular vortex trajectories determined from Fig. 8 equals $\Delta s \cong 10$ mm that for the velocity ratio $\varphi = C/U = 1$ and for cylinder diameter $d = 3$ mm gives the value of Strouhal number

$$St = \frac{d}{\Delta s\sqrt{1+\varphi^2}} \cong 0.2 \tag{4.2}$$

which is in a good agreement with earlier measurements performed by Bogusławski and Elsner [2] as well as with the results obtained by Wierciński [12]. Quite typical is also the decay of oscillatory motion at the distance $x/d > 8$ from the cylinder which results from the viscous destruction of the Karman vortex street.

It is worth noticing that the well defined vortical structures visible at the phase-averaged picture of velocity field, may be treated as a direct proof of the

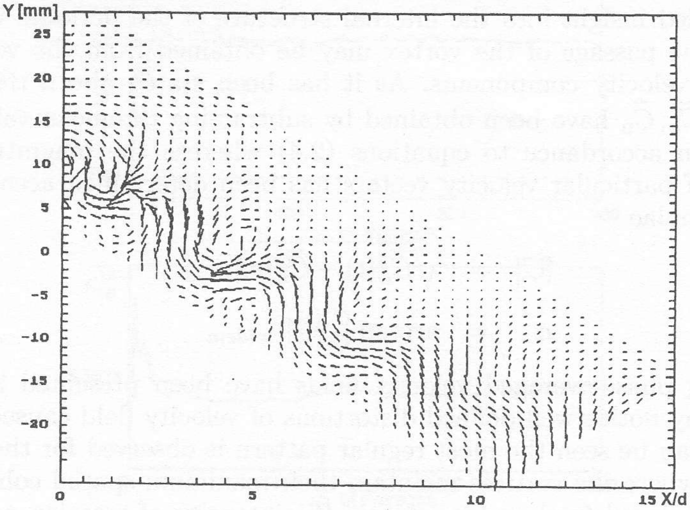

Fig. 8. The phase-averaged velocity field for phase $\tau = 0.45$ calculated according to (2.4).

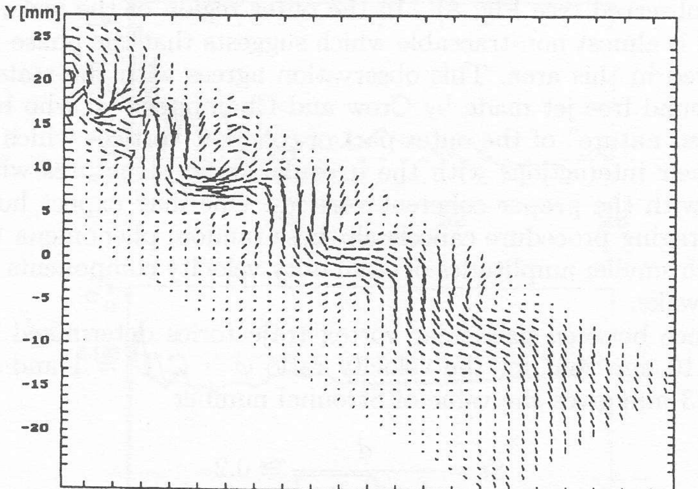

Fig. 9. The phase-averaged velocity field for phase $\tau = 0.55$ calculated according to (2.4).

synchronisation between the position of the wake and the Karman vortex street. The shape of the velocity field shown in Fig. 8 clearly proves that a moving circular cylinder entering the jet potential core generates the Karman vortex street in a repetitive manner, i.e. the first vortex in the flow field is formed always almost in the same place. The substantial length of oscillatory velocity components shown in Fig. 8 suggest that the contribution of vortex induced velocity field in a flow behind moving cylinder is quite significant.

More detailed information concerning the oscillatory velocity pattern induced in the wake by passing vortices may be obtained from the analysis of isolines of velocity modules calculated from eq. (4.1). Typical picture obtained for phases $\tau = 0.50$ and $\tau = 0.56$ have been presented in Figs. 10 and 11. The velocity modulus isolines indicate the areas of various intensity of velocity gradients characteristic for the Karman vortex street.

5. Vortex convection velocity in a flow field

Velocity fields presented in Figs. 8, 9 have been obtained only for the two, sample time stages of a moving Karman street. Taking under consideration all the available data it became possible to determine all positions of particular vortices in consecutive intervals of time, and in this way to find the vortex trajectories. Such trajectories are presented in Fig. 12, where one can easy see that trajectories at very close distance to the plane of a moving wheel $(0 < x/d < 3)$ have highly distorted shapes. The calculated points can be, however, approximated by straight lines of a stable slope for $x/d > 3$ and this observations proved that an assumption concerning the straight-line vortex trajectories, presented by Bogusławski and Elsner [2], was not preserved in the analysed flow. It should be noted however, that the particular points denoting the location of vortex centres in Fig. 12 have been determined as the location of the isoline maxima of velocity modulus. It is obvious that the points do not correspond to the velocity maxima and much better indication could be of course obtained from vorticity distributions. It was decided that such analysis will be performed in the near future.

The analysis of consecutive instantaneous velocity pictures obtained from the phase-averaged data enabled one to determine the vortex convection velocity which could be calculated as

$$W_c = (1 - k)W \tag{5.1}$$

where k is apriori unknown function of time. The convection velocity components in a stationary frame of reference might be expressed by

$$\begin{aligned} (C_u)_c &= -W_c \sin\alpha + U \\ (C_a)_c &= -W_c \cos\alpha \end{aligned} \tag{5.2}$$

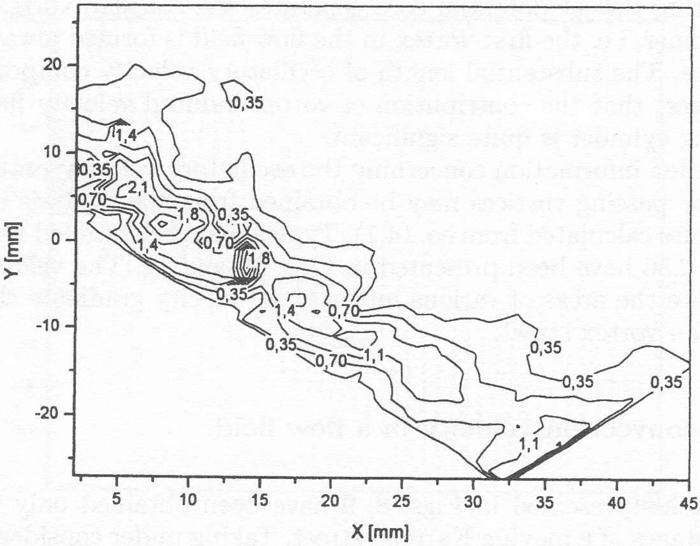

Fig. 10. Isoline contours of phase-averaged velocity modulus for phase $\tau = 0.45$.

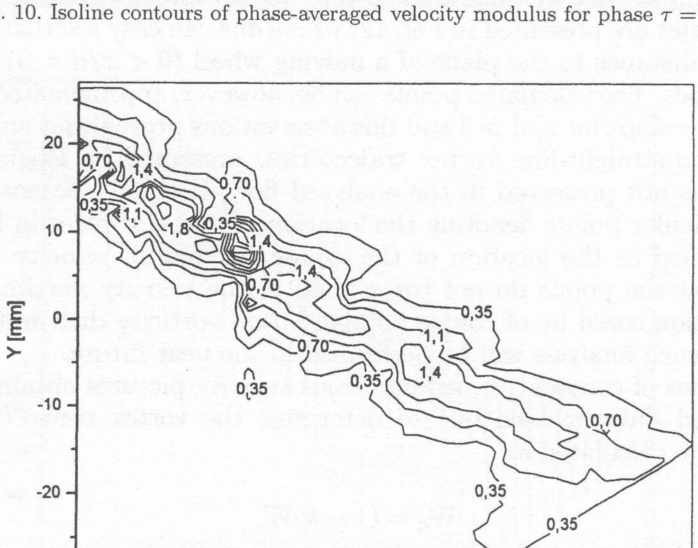

Fig. 11. Isoline contours of phase-averaged velocity modulus for phase $\tau = 0.55$.

Since

$$\begin{aligned} \sin\alpha &= \frac{U}{W} = \frac{U}{\sqrt{U^2+C^2}} = \frac{1}{\sqrt{1+\varphi^2}} \\ \cos\alpha &= \frac{C}{W} = \frac{C}{\sqrt{U^2+C^2}} = \frac{\varphi}{\sqrt{1+\varphi^2}} \end{aligned} \tag{5.3}$$

where velocity ratio $\varphi = C/U$ we finally have

$$(C_u)_c = kU; \quad (C_a)_c = (1-k)C \tag{5.4}$$

The corresponding value of coefficient k, according to Bogusławski and Elsner [2] could be calculated from the equation

$$k = \frac{\varphi \tan\beta}{1+\varphi\tan\beta} \tag{5.5}$$

where $\tan\beta$ is the slope of vortex trajectories. Analysis performed by Bogusławski and Elsner [2] allowed to assume the value of coefficient k equal 0.167 and in this way to apply the assumption concerning the constant convection velocity of Karman vortices.

Taking advantage of the fact that vortex trajectories are not straight lines (Fig. 12), at least in the distance $x/d < 3$, it was decided to calculate the value of coefficient k as a function of distance x. The results are presented in Fig. 13 where the dashed line represents k value taken after Bogusławski and Elsner [2]. It is clear that at very close area to moving cylinder, coefficient k attains high value 0.44 but in the downstream direction its value decreases very fast and converges to a level equal 0.167, which has been obtained among the others by Bogusławski and Elsner [2].

6. Concluding remarks

It may be concluded from the presented work that a moving circular cylinder entering the free stream through sharp jet velocity profile generates a Karman vortex street in repetitive manner, in which the first vortex in the flow field is formed always almost in the same place. The contribution of the vortex induced velocity field behind a moving cylinder is significant even in a quite far region from the plane determined by the passing cylinders. However, the trajectories of vortices are not straight lines especially just behind the cylinder, as it has been revealed by the varying value of coefficient k.

The final observation is, that experimental results registered in a phase-correlated wake may be strongly dependent on the location of measuring point, what may be of certain importance for modelling unsteady phenomena in fluid flow machinery.

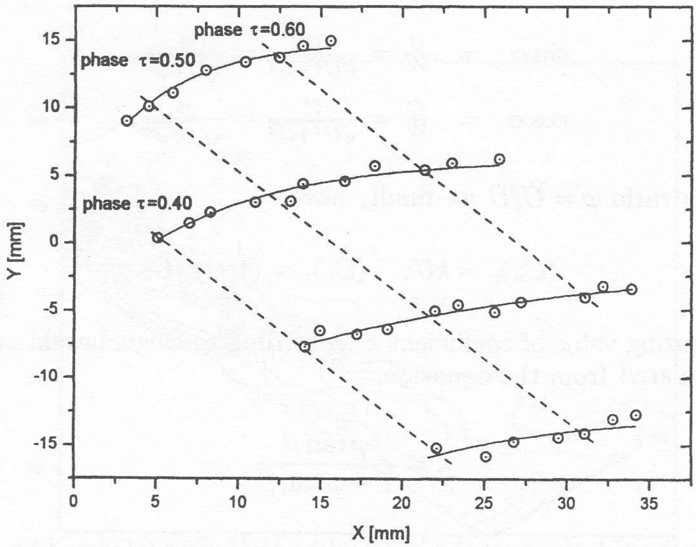

Fig. 12. Reconstruction of a set of vortex trajectories behind moving cylinder.

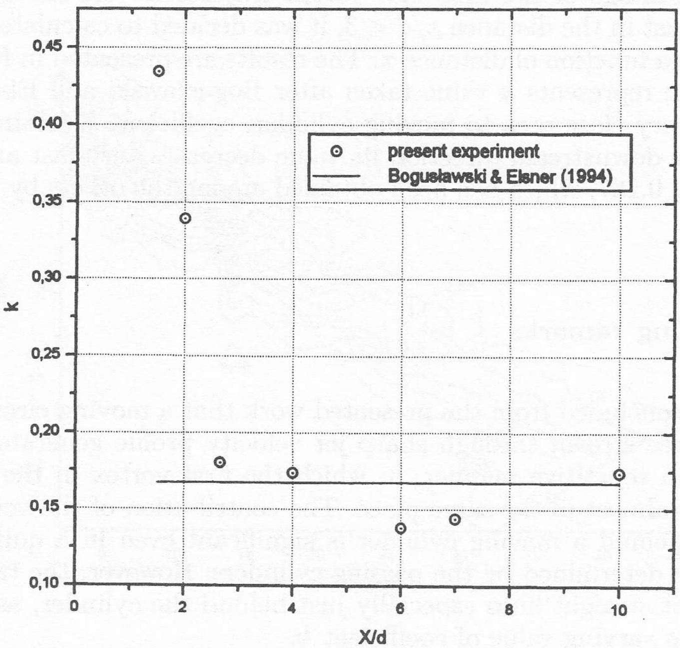

Fig. 13. Coefficient k as a function of a distance behind moving cylinder.

Ackowledgements This work was sponsored by a statutory funds BS-03-301/91 as well as BW-03-204/97 provided by the Institute of Thermal Machinery Technical University of Częstochowa.

Received in revised form 20 July 1998

References

[1] Adachi, T., Murakami, Y.: *Three-dimensional velocity distribution between stator blades and unsteady force on a blade due to passing wakes*, Bull. of ASME, vol. 22, no. 170, 1979, 1074-1082.

[2] Bogusławski, A., Elsner, J.W.: *Wake structure and vortex path behind the moving circular cylinder*, J.of Theoretical and Applied Mechanics 4, 32, 1994, 735-751.

[3] Bogusławski A., Drobniak S., Elsner W.: *Phase correlated vortex street in a moving cylinder wake*, Proc. of a Conference "Modeling and Design in Fluid-Flow Machinery", Gdańsk 1997, 377-382.

[4] Crow S.C., Champagne F.H.: *Orderly structure in a jet turbulence*, J. Fluid Mech., vol. 481971, 547-591.

[5] Dullenkopf, K., Schulz. A., Witting, S.: *Turbine airfoil heat transfer under simulated wake conditions*, Proc. of a Int. Symposium Heat Transfer in Turbomachinery, Athens, 1992, 1-14.

[6] Elsner, J.W.: *Turbulence in flows*, PWN Warszawa, 1987 (in Polish).

[7] Elsner, J.W., Bogusławski, A.: *Vortex street behind the rotating disc of circular cylinders*, Cieplne Maszyny Przepływowe, vol. 108, 105-113.

[8] Gallus, H.E., Schulz. H.D., Poensgen, G., Hönen H.: *Investigation of flow separation in axial-flow compressors*, Księga Jubileuszowa 70-lecia urodzin Prof. E.Tuliszki, Wydz. Maszyn Roboczych i Pojazdów Politechniki Poznańskiej, 1990, 103-128.

[9] Poensgen C., Gallus H.E.: *There dimensional wake decay inside of a compressor cascade and its influence on the downstream unsteady flow field. Part I – Wake decay characteristics in the flow passage*, Trans. ASME, J. of Turbomachinery, vol. 113(1991), 180-189.

[10] Schulz, H.D., Gallus, H.E., Lakshminarayana, B.: *Three-dimensional separated flow field in the endwall region of an annular compressor cascade in the presence of rotor-stator interaction: Part I – Quasi-steady slow field and comparison with steady-state data, Part II – Unsteady flow and pressure field*,

Trans. ASME, J. of Turbomachinery, vol. 112(1990), 669-678 (I), 679-690 (II).

[11] Wierciński Z.: *The influence of the wake structure on the dynamic blade load*, UAATP, 6th Int.Symp. Aachen , 1987.

[12] Wierciński Z.: *Geometry of vortex streets behind a moving palisade of cylinders*, IFFM PAS internal report, 280/1164/89, 1989, 3-24.

[13] Wood D.H., Peterson P.L., Clausen P.D.: *The turbulent wake of a circular cylinder rotating about the streamwise axis*, Exp. Fluids 16(1994), 375-384.

[14] Wysocki M., Drobniak S., Elsner W.: *Generation of flow periodicity in a wind-tunnel experiment*, J. of Theoretical and Applied Mechanics 2, 34, 475-488.

Fazowa rekonstrukcja śladu za poruszającym się cylindrem

Streszczenie

Przedmiotem pracy jest analiza oddziaływania śladu za poruszającym się cylindrem na pole prędkości na wlocie do kaskady kierowniczej. Pomiary prowadzone były przy wykorzystaniu aparatury termoanemometrycznej oraz techniki uśredniania fazowego, w której sygnał odniesienia wyzwalany był przez stałe położenie kątowe wirującego pręta. Jak stwierdzono, przepływ za poruszającym się cylindrem zdominowany jest przez powstające naprzemiennie wiry Karmana. Analiza uśrednionych fazowo pól prędkości potwierdziła tezę o synchronicznym formowaniu się ścieżki wirowej w momencie wejścia pręta w potencjalny rdzeń strugi kołowej.